

Astroglial CB₁ Receptors Determine Synaptic D-Serine Availability to Enable Recognition Memory

Highlights

- Astrocytes are important for long-term object recognition memory
- Astroglial CB₁ receptors are coupled to D-serine availability at synapses
- Appropriate D-serine levels are required for NMDAR activity and LTP induction

Authors

Laurie M. Robin,
José F. Oliveira da Cruz,
Valentin C. Langlais, ..., Aude Panatier,
Stéphane H.R. Oliet,
Giovanni Marsicano

Correspondence

giovanni.marsicano@inserm.fr

In Brief

Robin et al. show that astroglial CB₁ receptors in the hippocampus regulate D-serine supply to NMDA receptors, a process necessary for LTP induction and object recognition memory.



Astroglial CB₁ Receptors Determine Synaptic D-Serine Availability to Enable Recognition Memory

Laurie M. Robin,^{1,2,10} José F. Oliveira da Cruz,^{1,2,7,10} Valentin C. Langlais,^{1,2,10} Mario Martin-Fernandez,³ Mathilde Metna-Laurent,^{1,2,4} Arnau Busquets-Garcia,^{1,2} Luigi Bellocchio,^{1,2} Edgar Soria-Gomez,^{1,2,5,6} Thomas Papouin,^{1,2} Marjorie Varilh,^{1,2} Mark W. Sherwood,^{1,2} Ilaria Belluomo,^{1,2} Georgina Balcells,^{1,2} Isabelle Matias,^{1,2} Barbara Bosier,^{1,2} Filippo Drago,⁷ Ann Van Eeckhout,⁸ Ilse Smolders,⁸ Francois Georges,^{2,9} Alfonso Araque,³ Aude Panatier,^{1,2} Stéphane H.R. Oliet,^{1,2,11} and Giovanni Marsicano^{1,2,11,12,*}

¹INSERM U1215, NeuroCentre Magendie, 33077 Bordeaux, France

²University of Bordeaux, 33077 Bordeaux, France

³Department of Neuroscience, University of Minnesota, Minneapolis, MN 55455, USA

⁴Aelis Farma, 33077 Bordeaux, France

⁵Department of Neurosciences, University of the Basque Country UPV/EHU, 48940 Leioa, Spain

⁶KERBASQUE, Basque Foundation for Science, 48013 Bilbao, Spain

⁷Department of Biomedical and Biotechnological Sciences, Section of Pharmacology, University of Catania, 95123 Catania, Italy

⁸Vrije Universiteit Brussel, Department of Pharmaceutical Chemistry, Drug Analysis and Drug Information (FASC), Research group Experimental Pharmacology, Center for Neurosciences (C4N), Laarbeeklaan 103, 1090 Brussels, Belgium

⁹Centre National de la Recherche Scientifique, Neurodegenerative Diseases Institute, UMR 5293, 33076 Bordeaux, France

¹⁰These authors contributed equally

¹¹These authors contributed equally

¹²Lead Contact

*Correspondence: giovanni.marsicano@inserm.fr

<https://doi.org/10.1016/j.neuron.2018.04.034>

SUMMARY

Bidirectional communication between neurons and astrocytes shapes synaptic plasticity and behavior. D-serine is a necessary co-agonist of synaptic N-methyl-D-aspartate receptors (NMDARs), but the physiological factors regulating its impact on memory processes are scantily known. We show that astroglial CB₁ receptors are key determinants of object recognition memory by determining the availability of D-serine at hippocampal synapses. Mutant mice lacking CB₁ receptors from astroglial cells (GFAP-CB₁-KO) displayed impaired object recognition memory and decreased *in vivo* and *in vitro* long-term potentiation (LTP) at CA3-CA1 hippocampal synapses. Activation of CB₁ receptors increased intracellular astroglial Ca²⁺ levels and extracellular levels of D-serine in hippocampal slices. Accordingly, GFAP-CB₁-KO displayed lower occupancy of the co-agonist binding site of synaptic hippocampal NMDARs. Finally, elevation of D-serine levels fully rescued LTP and memory impairments of GFAP-CB₁-KO mice. These data reveal a novel mechanism of *in vivo* astroglial control of memory and synaptic plasticity via the D-serine-dependent control of NMDARs.

INTRODUCTION

The endocannabinoid system is an important modulator of physiological functions. It is composed of cannabinoid receptors, their endogenous ligands (i.e., endocannabinoids, eCB), and the enzymatic machinery responsible for their synthesis and degradation (Busquets-Garcia et al., 2018; Piomelli, 2003). The presence of type-1 cannabinoid receptors (CB₁) and the activity-dependent mobilization of endocannabinoids in different brain regions, including the hippocampus, are particularly involved in the modulation of several types of memory and associated cellular processes (Kano et al., 2009; Marsicano and Lafenêtre, 2009). Moreover, brain CB₁ receptors are expressed in different neuronal types, including inhibitory gamma-aminobutyric acid (GABA)ergic and excitatory glutamatergic neurons, where their stimulation negatively regulates the release of neurotransmitters (Kano et al., 2009).

CB₁ receptors are also expressed in glial cells, particularly astrocytes (Andrade-Talavera et al., 2016; Han et al., 2012; Min and Nevean, 2012; Navarrete and Araque, 2008; Rasooli-Nejad et al., 2014). For more than a century, astrocytes were thought to play an important supportive and nutritive role for neurons without actively participating in brain information processing (Allaman et al., 2011; Araque et al., 2014). However, it is now known that peri-synaptic astroglial processes surrounding pre- and postsynaptic neuronal elements form the so-called “tripartite synapse,” where astrocytes actively contribute to information processing (Araque et al., 2014; Perea et al., 2009).



In vivo and *in vitro* studies showed that astroglial CB₁ receptor signaling indirectly modulates glutamatergic transmission onto hippocampal pyramidal neurons (Han et al., 2012; Metna-Laurent and Marsicano, 2015; Navarrete and Araque, 2010; Oliveira da Cruz et al., 2016). For instance, the disruptive effect of exogenous cannabinoids on short-term spatial working memory is mediated by astroglial CB₁ receptors through an N-methyl-D-aspartate receptor (NMDAR)-dependent mechanism in the hippocampus (Han et al., 2012). Yet, the role of astroglial CB₁ receptors in physiological long-term memory processes and the precise mechanisms involved are still unknown (Metna-Laurent and Marsicano, 2015).

D-serine is the co-agonist of synaptic NMDARs and its action is required to induce different forms of synaptic plasticity (Henneberger et al., 2010; Panatier and Oliet, 2006; Panatier et al., 2006; Papouin et al., 2012, 2017b; Shigetomi et al., 2013; Sultan et al., 2015). Although the direct source of the amino acid is still under debate (Araque et al., 2014; Papouin et al., 2017c; Wolosker et al., 2016), there is convergent consensus that its supply to synapses requires Ca²⁺-dependent astrocyte activity (Araque et al., 2014; Papouin et al., 2017c; Wolosker et al., 2016). However, whether astroglial CB₁ receptors control the synaptic availability of D-serine during memory processing is not known.

Using genetic, behavioral, electrophysiological, imaging, and biochemical experimental approaches, in this study we asked whether the physiological activity of astroglial CB₁ receptors is involved in long-term object recognition memory and whether the mechanisms involved imply the regulation of glial-neuronal interactions. The results show that physiological activation of astroglial CB₁ receptors in the hippocampus is necessary for long-term object recognition memory consolidation via a mechanism involving the supply of D-serine to synaptic NMDARs and, consequently, the regulation of hippocampal synaptic plasticity. Thus, astroglial CB₁ receptors contribute to the time- and space-specific synaptic actions of astrocytes to promote memory formation.

RESULTS

Deletion of Hippocampal Astroglial CB₁ Receptors Impairs Object Recognition Memory and *In Vivo* NMDAR-Dependent LTP

To study the physiological role of astroglial CB₁ receptors in memory, we tested conditional mutant mice lacking CB₁ receptors in glial fibrillary acidic protein (GFAP)-positive cells (GFAP-CB₁-KO mice) (Han et al., 2012) in a long-term novel object recognition memory task in an L-maze (NOR) (Busquets-Garcia et al., 2011; Puighermanal et al., 2009, 2013). GFAP-CB₁-KO mice displayed a significant memory deficit as compared to their control littermates (Figure 1A; see also Figure S1A), with no alteration in total object exploration time (Figure S1B). Hippocampal NMDAR-dependent transmission is involved in many forms of memory (Kandel et al., 2002; Puighermanal et al., 2009; Warburton et al., 2013), yet the involvement of hippocampal NMDARs on NOR memory is still under debate, as it seems to depend on specific experimental conditions (Balderas et al., 2015; Warburton and Brown, 2015). To clarify this issue, we set to investigate where these receptors are required for NOR memory

formation in our behavioral paradigm. Intra-hippocampal administration of the NMDARs antagonist D-AP5 (15 μg/side; Figure S1C) fully abolished memory performance in wild-type (WT) mice when injected immediately after acquisition (Figure 1B; see also Figure S1D), but not 6 hr later (Figures S1F–S1H), with no alteration in total exploration time (Figure S1E). Thus, consolidation of long-term object recognition memory in the NOR task specifically requires astroglial CB₁ receptors and hippocampal NMDARs signaling.

Activity-dependent plastic changes of synaptic strength, such as NMDAR-dependent long-term potentiation (LTP), are considered cellular correlates of memory formation (Kandel et al., 2002; Whitlock et al., 2006). To study astroglial CB₁ receptor involvement in LTP, we recorded *in vivo* evoked field excitatory postsynaptic potentials (fEPSPs) in the hippocampal CA3-CA1 pathway of anesthetized WT and mutant mice. High-frequency stimulation (HFS) induced LTP in C57BL/6N mice (Figures 1C and 1D). The systemic administration of the NMDAR antagonist MK-801 (3 mg/kg, i.p.), which did not alter basal evoked fEPSPs (Figures S1I–S1K), fully blocked the induction of LTP (Figures 1C and 1D; Figures S1I–S1K), confirming its NMDAR dependency. Notably, this form of plasticity was abolished in GFAP-CB₁-KO mice as compared to their WT littermates (Figures 1E and 1F), showing that CB₁ receptors expressed in GFAP-positive cells are necessary for *in vivo* hippocampal NMDAR-dependent LTP induction. Altogether, these data demonstrate that astroglial CB₁ receptors are essential for hippocampal NMDAR-dependent object recognition memory and LTP.

Activation of CB₁ Receptors Increases Astroglial Ca²⁺ Levels and Extracellular D-Serine

Increase of astroglial intracellular Ca²⁺ modulates synaptic glutamatergic activity and plasticity via the release of gliotransmitters, whose identity likely depend on the brain region and the type of plasticity involved (Araque et al., 2014; Sherwood et al., 2017). Because activation of CB₁ receptors generate Ca²⁺ signals in astrocytes (Araque et al., 2014; Metna-Laurent and Marsicano, 2015; Oliveira da Cruz et al., 2016), the impaired object recognition memory and synaptic plasticity in GFAP-CB₁-KO mice might result from alterations of astroglial Ca²⁺ regulation of specific hippocampal gliotransmitters.

First, we tested whether the CB₁ receptor-dependent modulation of intracellular Ca²⁺ levels (Gómez-Gonzalo et al., 2015; Min and Nevian, 2012; Navarrete and Araque, 2008, 2010) depends on direct activation of astroglial CB₁ receptors. Local pressure application of the CB₁ receptor agonist WIN55,212-2 (WIN) induced a reliable increase of Ca²⁺ levels in somas and principal processes of hippocampal astrocytes in slices from GFAP-CB₁-WT mice (Figures 2A–2E). As expected (Gómez-Gonzalo et al., 2015; Min and Nevian, 2012; Navarrete and Araque, 2008, 2010), this effect was fully blocked by the CB₁ receptor antagonist AM251 (2 μM; Figures 2B–2E). Notably, WIN had no effect in slices from GFAP-CB₁-KO littermates (Figures 2B–2E), clearly indicating the direct impact of astroglial CB₁ receptor activation on intracellular Ca²⁺ levels.

Via Ca²⁺-dependent mechanisms, astrocytes can promote the synaptic release of several signaling molecules known as gliotransmitters (Araque et al., 2014). One of them is D-serine, which

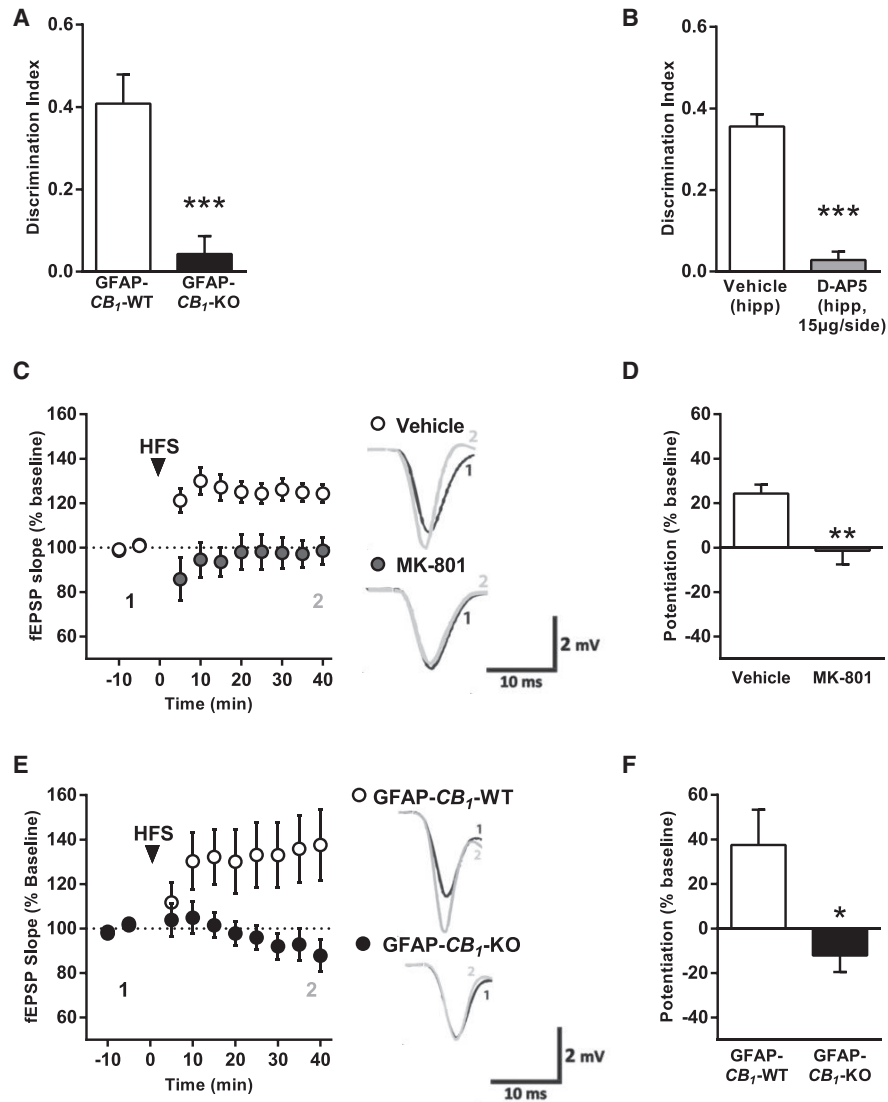


Figure 1. Hippocampal Astroglial CB₁ Receptors Are Necessary for NMDAR-Dependent Object Recognition Memory and *In Vivo* LTP

(A) Memory performance of GFAP-CB₁-WT mice (n = 10) and GFAP-CB₁-KO littermates (n = 11) in the NOR task.

(B) Effects of intra-hippocampal infusions of vehicle (n = 10) or D-AP5 (15 µg/side; n = 8) on NOR performance.

(C and D) High-frequency stimulation in the CA3 area of hippocampus induces NMDAR-dependent LTP in CA1 stratum radiatum. (C) Summary plots of normalized fEPSPs in anesthetized mice under vehicle (n = 6) or MK-801 treatment (3 mg/kg; i.p.; n = 5). (D) Bar histograms of normalized fEPSPs from experiment in (C), 40 min after HFS.

(E and F) *In vivo* LTP is absent in GFAP-CB₁-KO mice. (E) Summary plots of normalized fEPSPs in GFAP-CB₁-WT (n = 9) and GFAP-CB₁-KO (n = 6) littermates. (F) Bar histograms of normalized fEPSPs from experiment in (E), 40 min after HFS. Traces on the right side of the summary plots in (C) and (E) represent 150 superimposed evoked fEPSPs before (1, black) and after (2, gray) HFS.

Data, mean ± SEM. *p < 0.05, **p < 0.01, ***p < 0.001.

See also Figure S1 and Table S1.

plays a key role in NMDAR signaling (Araque et al., 2014). Therefore, we asked whether activation of CB₁ receptors might modulate the release of this amino acid. Application of WIN (5 µM) to hippocampal slices did not alter the tissue levels of several amino acids (Figures S2A–S2D). However, the same treatment slightly but specifically increased the extracellular levels of D-serine (Figures 2F–2I), indicating that activation of astroglial CB₁ receptors can control the release of this signaling amino

acid, a process that depends on intracellular Ca²⁺ signaling (Bohmbach et al., 2018; Henneberger et al., 2010).

Astroglial CB₁ Receptor-Mediated D-Serine Supply Is Required for Hippocampal LTP

D-serine is the co-agonist of hippocampal synaptic NMDARs and its presence is necessary for LTP induction (Bohmbach et al., 2018; Henneberger et al., 2010; Papouin et al., 2012).

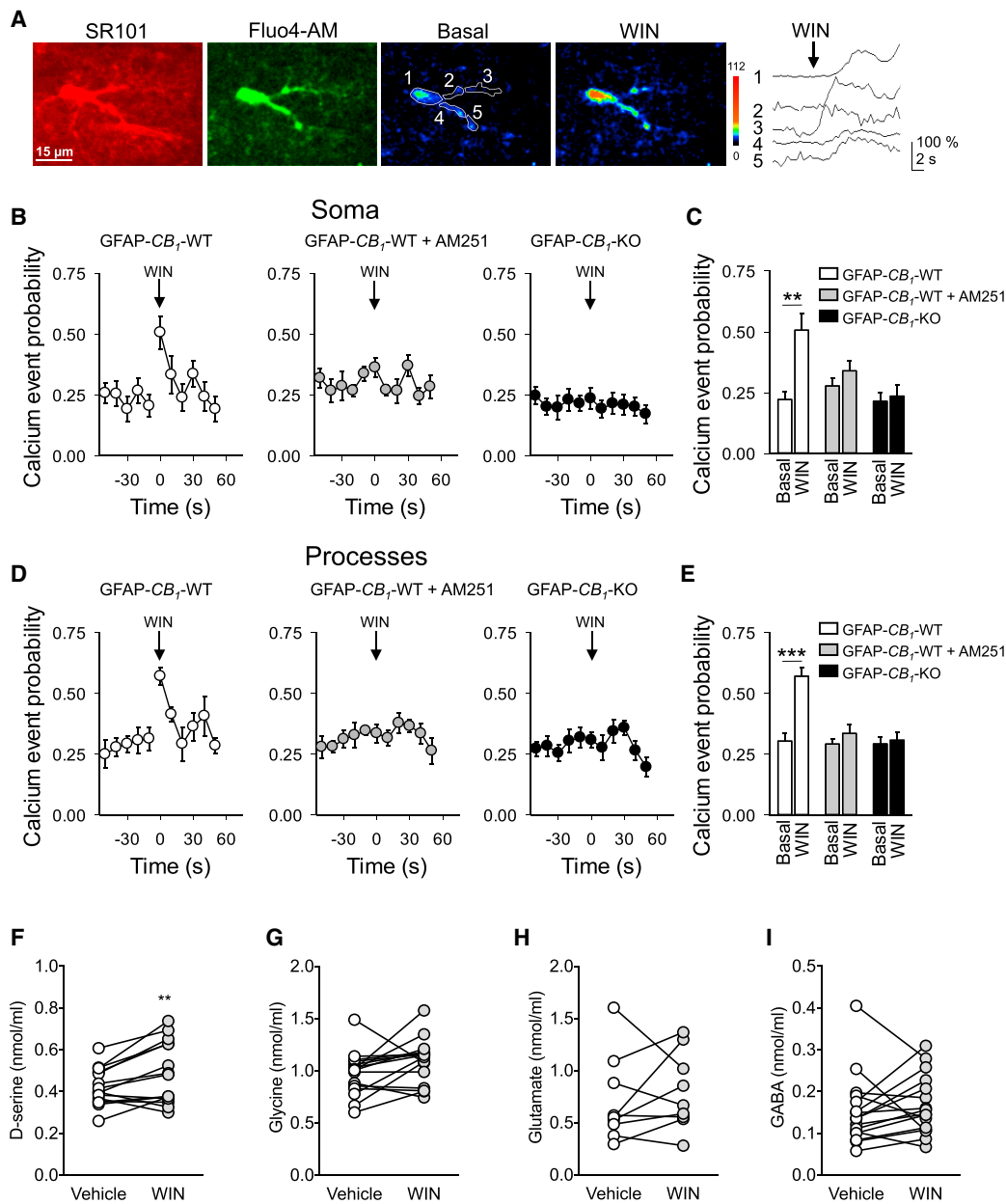


Figure 2. Activation of Astroglial CB_1 Receptors Enhances Intracellular Ca^{2+} Levels in Astrocytes and Extracellular D-Serine

(A) Representative image of a hippocampal astrocyte stained with SR101 and Fluo4 and pseudo-color images representing fluorescence intensities before and after WIN 515,212-2 (WIN) application, with the correspondent Ca^{2+} traces (numbers refer to different subcellular locations on the astrocyte).

(B) Somatic calcium event probability before and after WIN (at time = 0) in GFAP- CB_1 -WT in control conditions (white), in the presence of AM251 (2 μ M; gray), and in GFAP- CB_1 -KO mice (black).

(C) Somatic calcium event probability before and after WIN in GFAP- CB_1 -WT in control conditions (white; n = 9 slices and 79 somas), in the presence of AM251 (gray; n = 12 slices and 159 somas), and in GFAP- CB_1 -KO mice (black; n = 16 slices and 145 somas).

(D) Calcium event probability in the processes before and after WIN (at time = 0) in GFAP- CB_1 -WT in control conditions (white), in the presence of AM251 (2 μ M; gray), and in GFAP- CB_1 -KO mice (black).

(E) Calcium event probability in the processes before and after WIN in GFAP- CB_1 -WT in control conditions (white; n = 8 slices and 171 processes), in the presence of AM251 (gray; n = 8 slices and 140 processes), in GFAP- CB_1 -KO mice (black; n = 10 slices and 189 processes).

(F–I) Determination of D-serine (F), glycine (G), glutamate (H), and GABA (I) as measured by capillary electrophoresis in extracellular solutions of acute mouse hippocampal slices treated with vehicle or WIN.

Data, mean \pm SEM. *p < 0.05, **p < 0.01, ***p < 0.001.

See also Figure S2 and Table S1.

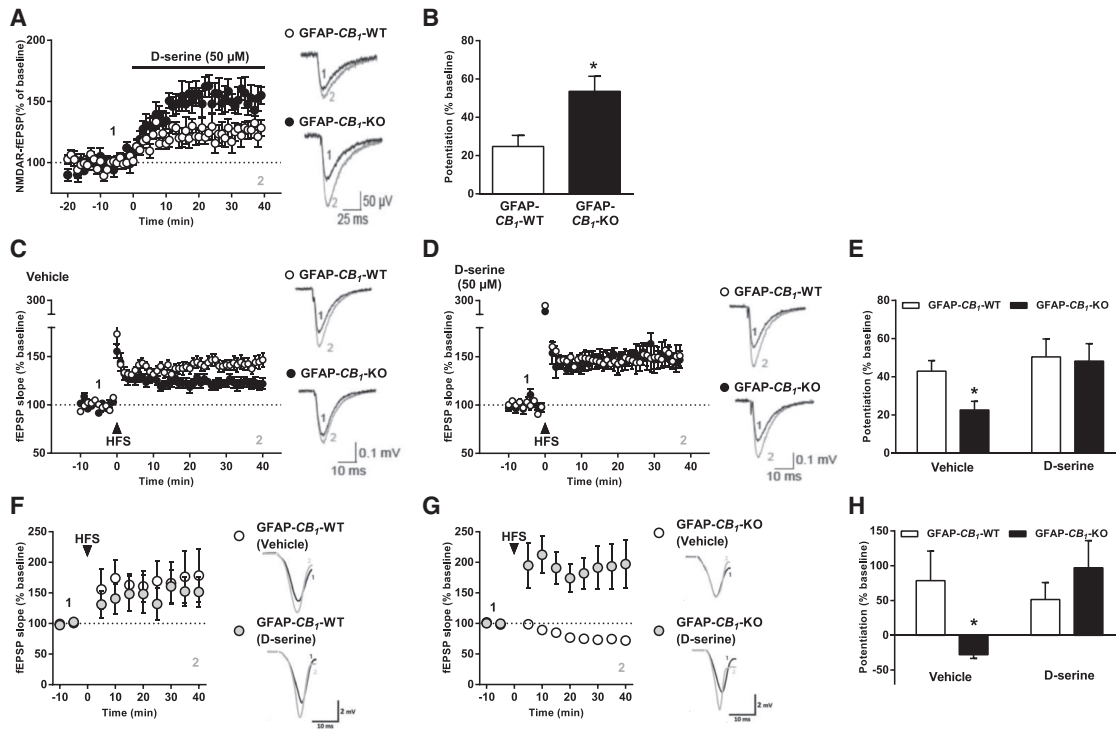


Figure 3. Astroglial CB₁ Receptors Control LTP Induction through D-Serine

(A) Summary plots showing the effect of D-serine application on NMDAR co-agonist binding site occupancy in slices from GFAP-CB₁-WT mice and GFAP-CB₁-KO littermates. Traces represent 60 superimposed NMDAR-fEPSPs before (1, black) and after (2, gray) D-serine application.

(B) Bar histograms of normalized NMDAR-fEPSPs from experiment in (A) measured 20–40 min after D-serine application.

(C) *In vitro* LTP is impaired in GFAP-CB₁-KO mice. Summary plots of normalized fEPSPs in slices from GFAP-CB₁-WT (n = 16) and GFAP-CB₁-KO (n = 12) mice before (1) and after (2) high-frequency stimulation (HFS).

(D) D-serine application rescues LTP in slices from GFAP-CB₁-KO mice. Summary plots of fEPSPs showing the effect of D-serine (50 μM) on LTP in slices from GFAP-CB₁-WT (n = 8) and GFAP-CB₁-KO (n = 7) mice.

In (C) and (D), traces represent 30 superimposed successive fEPSPs before (1, black) and after (2, gray) the HFS stimulation (arrow).

(E) Bar histograms of fEPSPs from experiments in (C) and (D) measured 30–40 min after HFS.

(F and G) Summary plots of normalized fEPSPs in GFAP-CB₁-WT (F) and GFAP-CB₁-KO (G) treated with vehicle (GFAP-CB₁-WT, n = 4; GFAP-CB₁-KO, n = 7) or D-serine (GFAP-CB₁-WT, n = 6; GFAP-CB₁-KO, n = 5). In (F) and (G), traces represent 150 superimposed successive fEPSPs before (1, black) and after (2, gray) the HFS stimulation (arrow).

(H) Bar histograms of normalized fEPSPs from experiment in (F) and (G), 40 min after HFS.

Data, mean ± SEM. *p < 0.05.

See also [Figure S3](#) and [Table S1](#).

Thus, astroglial CB₁ receptors might control the activity of NMDARs and hippocampal LTP by regulating the synaptic levels of D-serine. Measurements of bulk extracellular amino acids as performed in [Figures 2F–2I](#) do not specifically address whether D-serine levels impact synaptic function. A direct way to evaluate the levels and functions of synaptic D-serine is to perform electrophysiological measurements to assess the occupancy of the NMDAR co-agonist binding site at CA3-CA1 synapses ([Papouin et al., 2012](#)). Thus, we measured the impact of exogenous applications of the D-serine on NMDAR-mediated fEPSPs at CA3-CA1 synapses in acute hippocampal slices ([Papouin et al., 2012](#)). Bath application of D-serine (50 μM) increased NMDAR-dependent synaptic responses in both GFAP-CB₁-WT and GFAP-CB₁-KO mice ([Figures 3A and 3B](#)). Strikingly, the effect of D-serine was twice more pronounced in the absence of astroglial CB₁ receptors ([Figures 3A and 3B](#)), indicating that these receptors are necessary to maintain appropriate concen-

trations of D-serine within the synaptic cleft and consequently ensuring a proper level of occupancy of the NMDAR co-agonist binding site.

Next, we asked whether astroglial CB₁ receptor-dependent release of D-serine controls synaptic plasticity by regulating NMDAR activity. First, *in vitro* electrophysiological recordings of fEPSPs at CA3-CA1 synapses in hippocampal slices revealed that GFAP-CB₁-WT and GFAP-CB₁-KO have comparable input-output relationships ([Figure S3A](#)), indicating that the deletion of astroglial CB₁ receptors did not alter basal glutamatergic synaptic transmission. HFS is known to induce endocannabinoid mobilization through the activation of mGluR1/5 receptors, eventually leading to long-term depression of inhibitory transmission (I-LTD) in the hippocampus ([Castillo et al., 2012](#); [Chevalleyre and Castillo, 2003](#)). Therefore, we asked whether mGluR1/5 receptors could be involved in HFS-induced LTP. Application of the mGluR1/5 antagonists LY367385 and MTEP,

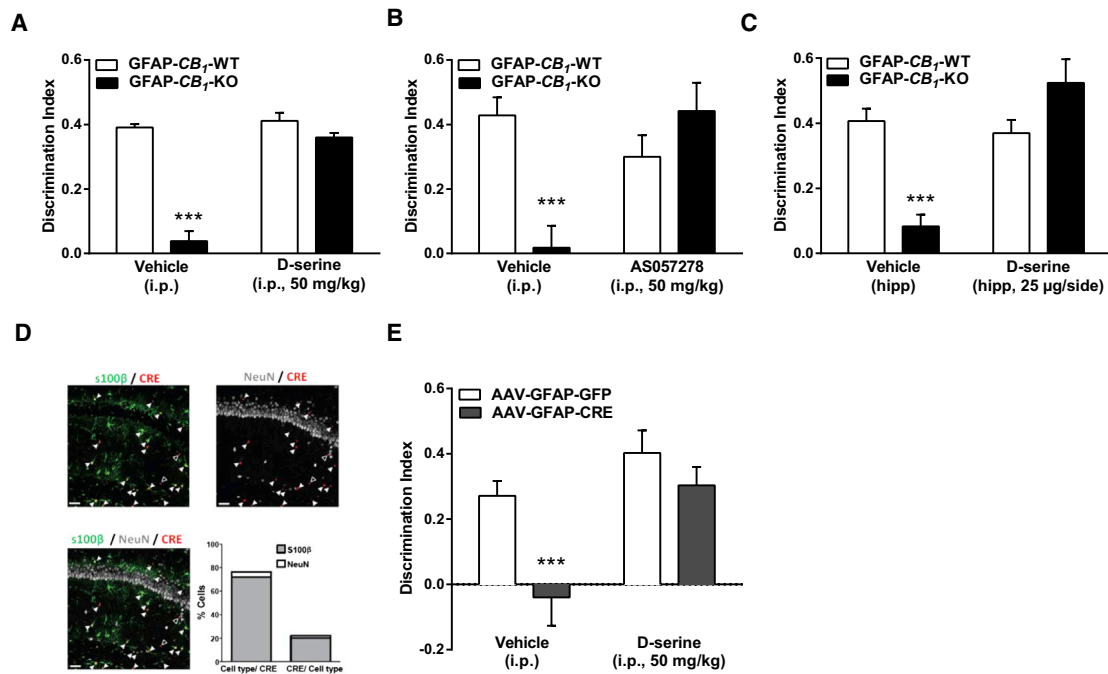


Figure 4. Hippocampal Astroglial CB_1 Receptors Are Necessary for Object Recognition Memory through D-Serine

(A) Memory performance of GFAP-*CB₁*-WT and GFAP-*CB₁*-KO mice injected with vehicle (n = 5 both groups) or D-serine (50 mg/kg; i.p.; GFAP-*CB₁*-WT, n = 4; GFAP-*CB₁*-KO, n = 5).

(B) Memory performance of GFAP-*CB₁*-WT and GFAP-*CB₁*-KO mice injected with vehicle (GFAP-*CB₁*-WT, n = 8; GFAP-*CB₁*-KO, n = 9) or AS057278 (50 mg/kg; i.p.; GFAP-*CB₁*-WT, n = 9; GFAP-*CB₁*-KO, n = 8).

(C) Memory performance of GFAP-*CB₁*-WT and GFAP-*CB₁*-KO mice intra-hippocampally injected with vehicle (GFAP-*CB₁*-WT, n = 5; GFAP-*CB₁*-KO, n = 7) or D-serine (25 μg/side; GFAP-*CB₁*-WT, n = 5; GFAP-*CB₁*-KO, n = 7).

(D) Immunofluorescence for s100β (green) and NeuN (white) in the hippocampus of mice injected with AAV-GFAP-CRE-mCherry (red). Filled arrows, cells co-expressing s100β and CRE. Empty arrows, cells expressing only CRE. Scale bar, 50 μM. Bottom right: quantification of co-expression indicating the percentage of neurons (NeuN-positive) and astrocytes (s100β positive) containing CRE recombinase over the total CRE-positive cells (left superposed bars) and the percentage of CRE-positive cells over the whole population of neurons and astrocytes (right superposed bars). Data are from 2–3 sections per animal from 8 mice injected with AAV-GFAP-CRE.

(E) Memory performance of *CB₁*-flox mice intra-hippocampally injected with either an AAV-GFAP-GFP or an AAV-GFAP-CRE and treated with vehicle (AAV-GFAP-GFP, n = 6; AAV-GFAP-CRE, n = 8) or D-serine (50 mg/kg; i.p.; AAV-GFAP-GFP, n = 7; AAV-GFAP-CRE, n = 8).

Data, mean ± SEM. ***p < 0.001.

See also Figure S4 and Table S1.

respectively, did not alter LTP (Figures S3B and S3C), suggesting that mGluR1/5 receptors are not involved in this process. Similarly to *in vivo* electrophysiological results, HFS-induced LTP was significantly reduced in GFAP-*CB₁*-KO mice as compared to GFAP-*CB₁*-WT (Figure 3C). Whereas the exogenous application of D-serine (50 μM) had no effect in slices from GFAP-*CB₁*-WT mice, it fully rescued *in vitro* LTP in GFAP-*CB₁*-KO littermates (Figures 3D and 3E). Importantly, the lack of *in vivo* LTP observed in GFAP-*CB₁*-KO was fully restored by the systemic administration of D-serine (50 mg/kg, i.p.; Figures 3F–3H).

Considering that activation of astroglial CB_1 receptors increases Ca^{2+} in astrocytes, we asked whether this subpopulation of cannabinoid receptors is involved in the HFS-induced regulation of astroglial Ca^{2+} dynamics (Perea and Araque, 2005; Porter and McCarthy, 1996; Sherwood et al., 2017). While the Ca^{2+} activity evoked in both soma and large processes of astrocytes during the HFS was the same, GFAP-*CB₁*-KO astro-

cytes displayed a reduction in the Ca^{2+} event probability after the HFS as compared to WT littermates (Figures S3D–S3J). Altogether, these results show that astroglial CB_1 receptors regulate Ca^{2+} dynamics in astrocytes and determine the synaptic levels of the NMDAR co-agonist D-serine necessary for NMDAR-dependent *in vitro* and *in vivo* LTP.

Astroglial CB_1 Receptors Determine NOR Memory via D-Serine

If, as shown above, astroglial CB_1 receptors determine the activity of NMDARs via the control of synaptic D-serine levels, this mechanism might underlie the processing of NOR memory. Strikingly, a sub-effective dose of D-serine (i.e., having no effect on memory performance per se, 50 mg/kg, i.p.; Figure S4A) reverted the memory impairment of GFAP-*CB₁*-KO mice (Figure 4A; see also Figures S4B and S4C). This effect of D-serine in GFAP-*CB₁*-KO mice was not present when the injection occurred 1 hr after acquisition or immediately before test

(Figures S4D and S4E), indicating that only the initial phase of NOR memory consolidation is altered in the mutant mice. Notably, administration of a sub-effective dose (Figure S4F) of the inhibitor of D-amino-acid oxidase AS057278 (50 mg/kg, i.p.), which increases endogenous D-serine levels *in vivo* (Adage et al., 2008), also rescued the phenotype of GFAP-*CB₁*-KO mice (Figure 4B; see also Figures S4G and S4H). Moreover, post-acquisition (i.e., after training phase) intra-hippocampal injections of D-serine (sub-effective dose of 25 μg/side; Figure S4I) also restored NOR memory performance in GFAP-*CB₁*-KO mice (Figure 4C; see also Figures S4J and S4K). This suggests that the hippocampus is the brain region where astroglial *CB₁* receptors control NMDAR-dependent memory formation via D-serine signaling. GFAP-*CB₁*-KO mice, however, carry a deletion of the *CB₁* gene in GFAP-positive cells in different brain regions (Bosier et al., 2013; Han et al., 2012), leaving the possibility that D-serine signaling in the hippocampus is remotely altered by deletion of astroglial *CB₁* receptors elsewhere. To specifically delete the *CB₁* gene in hippocampal astrocytes, we injected an adeno-associated virus expressing the CRE recombinase under the control of the GFAP promoter (AAV-GFAP-CRE-mCherry) or a control AAV-GFAP-GFP into the hippocampi of mice carrying the “floxed” *CB₁* receptor gene (Marsicano et al., 2003) (Figure 4D). Mice injected with the CRE recombinase were impaired in NOR memory performance (Figure 4E; see also Figures S4L and S4M), and notably, the systemic injection of D-serine (50 mg/kg, i.p.) fully reversed this phenotype (Figure 1E; see also Figures S4L and S4M). Thus, hippocampal astroglial *CB₁* receptors are required for NOR memory performance via the control of D-serine signaling during the initial phase of memory consolidation.

DISCUSSION

These results show that astroglial *CB₁* receptors are key determinants of physiological consolidation of object recognition memory in the hippocampus. Via Ca^{2+} -dependent mechanisms, they provide the synaptic D-serine levels required to functionally activate NMDARs and to induce LTP in the hippocampal CA1 region. In turn, this process is necessary upon learning to consolidate long-term object recognition memory (Figure S5). By causally linking the functions of a specific subpopulation of *CB₁* receptors, astroglial control of NMDAR activity via the gliotransmitter D-serine, and synaptic plasticity, these data provide an unforeseen physiological mechanism underlying memory formation.

By showing that astroglial *CB₁* receptors play a key role in the maintenance of the basal levels of D-serine in the synaptic cleft and thus in the control of NMDAR activity, these data shed light onto the pathway underpinning D-serine availability at synapses. Interestingly, it has been recently demonstrated that the amount of D-serine available during wakefulness depends on the activity of cholinergic fibers from the medial septum (Papouin et al., 2017b). Thus, synaptic D-serine levels are under the control of at least two sets of astroglial receptors, namely *CB₁* (present data) and $\alpha 7$ -nicotinic acetylcholine receptors (Papouin et al., 2017b).

Astrocytes occupy non-overlapping domains of the neuropil, where they survey the activity of thousands of synapses (Bushong et al., 2002; Pannasch and Rouach, 2013; Papouin et al.,

2017a). On the other hand, endocannabinoids are locally mobilized at synapses in an activity-dependent manner, and their actions are rather limited in space and time (Castillo et al., 2012; Kano et al., 2009; Piomelli, 2003). Therefore, it is tempting to speculate that astroglial *CB₁* receptors may act as sensors integrating the overall intensity of local synaptic activity within the territory of specific astrocytes, and this information may then be used to adjust the availability of D-serine and the activity of NMDARs. In this context, we propose that the astroglial *CB₁*-dependent regulation of D-serine supply is a major mechanism determining how much D-serine each astrocyte contributes to NMDARs as a function of neuronal activity within its territory.

Astroglial *CB₁* receptors have so far been described to impact synaptic plasticity in different ways. For instance, their activation by exogenous cannabinoids can promote NMDAR-dependent hippocampal LTD (Han et al., 2012), whereas their endogenous stimulation can, depending on experimental conditions, lead to heterosynaptic potentiation in the hippocampus, amygdala, and striatum (Martín et al., 2015; Martín-Fernández et al., 2017; Navarrete and Araque, 2008, 2010); spike-timing depression in the neocortex (Min and Nevian, 2012); or hippocampal LTP (present results). The conditions through which the activation of astroglial *CB₁* receptors might lead to different synaptic effects are currently not known (Araque et al., 2017; Metna-Laurent and Marsicano, 2015; Oliveira da Cruz et al., 2016). Future studies will surely reveal novel functions of astroglial *CB₁* receptors and will hopefully determine the physiological conditions and the cellular mechanisms leading to different forms of synaptic plasticity. In this context, the present data extend the value of astroglial *CB₁* receptors to the processing of object recognition memory through the regulation of D-serine, a key astrocyte-dependent modulator of synaptic functions.

The direct release of D-serine by astrocytes has recently been questioned, suggesting that astrocytes release L-serine, which, in turn, shuttles to neurons to fuel the neuronal synthesis of D-serine (Wolosker et al., 2016). Our data do not directly address this issue, but they support the idea that astrocyte functions and synaptic D-serine actions are required for hippocampal LTP (Henneberger et al., 2010; Papouin et al., 2017b, 2017c; Sherwood et al., 2017; Wolosker et al., 2016). Activation of hippocampal *CB₁* receptors by the agonist WIN induces a slight but significant increase of extracellular D-serine levels, which is specific among different amino acids. No clear evidence is currently present to explain the relative low amplitude of this pharmacological effect. However, it is possible that bulk measurement of amino acids lacks the power to detect specific changes at synaptic level. Unfortunately, it is currently technically impossible to obtain synaptic extracellular samples to directly measure amino acids in these tiny volumes. For this reason, we implemented another direct and reliable measure of synaptic D-serine levels by assessing the occupancy of synaptic NMDAR co-agonist sites (Henneberger et al., 2010; Papouin et al., 2012). The results clearly show that the occupancy of synaptic NMDAR co-agonist sites by D-serine is strongly reduced (more than 50%) in GFAP-*CB₁*-KO mice. HFS-induced LTP is fully abolished in GFAP-*CB₁*-KO mice *in vivo* but only partially reduced in *ex vivo* hippocampal slices. These slight discrepancies are likely due to uncontrollable factors that are necessarily different between

in vivo and *ex vivo* experimental conditions (Andersen, 2007; Windels, 2006), such as, for instance, the inevitable disruption of astroglial networks during slicing procedures or others. Importantly, however, the exogenous application of D-serine at the same doses, respectively, restoring learning *in vivo* and revealing the decrease of NMDAR occupancy in slices rescues LTP in both experimental settings. Thus, independently of their direct source, synaptic D-serine levels are under the control of CB₁ receptors specifically expressed in astrocytes, whose activation increases astroglial Ca²⁺ levels and promotes D-serine occupancy of synaptic NMDARs, eventually controlling specific forms of *in vivo* and *in vitro* LTP and object recognition memory.

Generalized activation or inhibition of CB₁ receptors does not reliably reflect the highly temporally- and spatially-specific physiological functions of the endocannabinoid system (Busquets-Garcia et al., 2018). Indeed, previous data showed that deletion of astroglial CB₁ receptors abolishes the impairment of hippocampal working memory by cannabinoid agonists, but it does not alter this form of short-term memory per se (Han et al., 2012), thereby leaving open the question of the physiological roles of astroglial CB₁ receptors in the hippocampus (Metna-Laurent and Marsicano, 2015; Oliveira da Cruz et al., 2016). This question could not be addressed using global genetic or pharmacological inactivation of CB₁ receptors, because it is known that CB₁ receptors expressed in different cellular subpopulations have often very diverse and even opposite impact on brain functions (Busquets-Garcia et al., 2016; Busquets-Garcia et al., 2015, 2018), and this is particularly true between neurons and astroglial cells (Busquets-Garcia et al., 2018; Metna-Laurent and Marsicano, 2015; Oliveira da Cruz et al., 2016). Indeed, global pharmacological activation, blockade, and genetic deletion of CB₁ receptors are not able to catch subtle but important effects of endocannabinoid signaling. For instance, recent data show that deletion of the CB₁ gene in hippocampal GABAergic or glutamatergic neurons induces decreased and increased *in vitro* LTP, respectively, as compared to WT mice (Monory et al., 2015), suggesting that results obtained by global receptor manipulation might be confounded by contrary physiological functions of cell-type-specific subpopulations of CB₁ receptors. Thus, the present results determine an unforeseen link between endogenous activation of astroglial CB₁ receptor signaling and long-term memory consolidation. Moreover, by showing the involvement of D-serine and NMDAR in these processes, our data provide an unexpected synaptic mechanism for this physiological function.

The deletion of the CB₁ gene in our study is induced in adult mice by tamoxifen treatment of GFAP-CB₁-KO mice or local injection of AAV-Cre under the control of a GFAP promoter into the hippocampus of CB₁-flox mice. These procedures occur a few weeks before testing, excluding potential compensatory confounding events during pre- and post-natal development. Moreover, the phenotypes of GFAP-CB₁-KO mice in NOR and LTP are rescued by increasing D-serine-dependent NMDAR signaling at the moment of memory acquisition/early consolidation or electrophysiological analysis. In particular, the behavioral effects of D-serine were present when it was administered systemically or locally immediately after task acquisition, but not 1 hr later or at recall. Thus, considering pharmacokinetic studies showing that the extracellular levels of D-serine are increased after exog-

enous administration for about 100 min in the brain (Fukushima et al., 2004), it is reasonable to conclude that the control of synaptic NMDAR plasticity and of NOR memory by astroglial CB₁ receptors is due to acute alterations of hippocampal circuitries during memory formation and LTP induction. An additional potential confounding factor is the role played by both D-serine (Sultan et al., 2015) and CB₁ receptors (Galve-Roperh et al., 2007) on adult neurogenesis. Due to the expression of GFAP in precursor neurons, we cannot fully exclude that neurogenesis might play a role in the mechanisms described. However, CB₁ receptors expressed in GFAP-positive cells are necessary for LTP at CA3-CA1 hippocampal synapses that are likely not influenced by neurogenesis events, which are known to specifically impact dentate gyrus circuits (Massa et al., 2011).

The role of CB₁ receptors expressed in GFAP-positive cells in NOR appears to be limited to the early phases of memory processing, namely early consolidation. Indeed, whereas the injection of D-serine immediately after memory acquisition fully rescues the phenotype of GFAP-CB₁-KO mice in NOR, the same treatment as soon as 1 hr after or just before memory retrieval has no effect. This is notable because it indicates a very early engagement of astrocyte signaling in memory processing, underlying the importance of glial-neuronal interactions at crucial phases of cognitive processes.

In conclusion, our data provide a novel neurobiological frame, in which the tight interaction between astrocytes and neurons required for the formation of object recognition memory is under the control of astroglial CB₁ receptors. Thus, by determining the physiological availability of D-serine at NMDARs, astroglial CB₁ receptors are key causal elements of spatial and temporal regulation of glia-neuron interactions underlying synaptic plasticity and cognitive processes in the brain.

STAR★METHODS

Detailed methods are provided in the online version of this paper and include the following:

- KEY RESOURCES TABLE
- CONTACT FOR REAGENT AND RESOURCE SHARING
- EXPERIMENTAL MODEL AND SUBJECT DETAILS
 - Animals
- METHOD DETAILS
 - Drug Preparation and Administration
 - Intra-hippocampal Drug Delivery
 - Viral Vectors, Intra-hippocampal Delivery, and Histological Verification
 - Novel Object Recognition Memory Task
 - *In Vivo* Electrophysiology
 - *In Vitro* Electrophysiology
 - Ca²⁺ Imaging
 - Measurement of Amino Acids in Hippocampal Slices
- QUANTIFICATION AND STATISTICAL ANALYSIS

SUPPLEMENTAL INFORMATION

Supplemental Information includes five figures and one table and can be found with this article online at <https://doi.org/10.1016/j.neuron.2018.04.034>.

ACKNOWLEDGMENTS

We thank Nathalie Aubailly, Magali Dubuc, and all the personnel of the Animal Facility of the NeuroCentre Magendie for mouse care. We thank Delphine Gonzales and all the personnel of the Genotyping Facility of the NeuroCentre Magendie. We thank the Histology and Biochemistry platforms of the NeuroCentre Magendie for help in the experiments. We thank also C. De Rijck (Vrije Universiteit Brussel) for help with experiments, and all the members of Marsicano's lab for useful discussions. This work was supported by INSERM (G.M. and S.H.R.O.), CNRS (S.H.R.O. and A.P.), EU-Fp7 (PAINCAGE, HEALTH-603191, G.M.), European Research Council (Endofood, ERC-2010-StG-260515 and CannaPreg, ERC-2014-PoC-640923, G.M.), Fondation pour la Recherche Médicale (DRM20101220445 and DPP20151033974, G.M.; FDT20160435664, J.F.O.d.C.; DEQ 20130326519, S.H.R.O.; FDT20150532252, V.C.L.), Human Frontiers Science Program (RGP0036//2014, G.M. and A.A.), Region Aquitaine (G.M.), Agence Nationale de la Recherche (ANR Blanc NeuroNutriSens ANR-13-BSV4-0006, G.M., and BRAIN ANR-10-LABX-0043, G.M., S.H.R.O., L.M.R., Animal Facility, Genotyping Facility, Histology Platform, and Biochemistry Platform), Fyssen Foundation and CONACyT (E.S.-G.), EMBO and FRM post-doc fellowships (L.B.), and French Ministry of Higher Education and Research (L.M.R. and V.C.L.).

AUTHOR CONTRIBUTIONS

L.M.R., J.F.O.d.C., and V.C.L. performed behavioral, *in vivo* electrophysiology, and *in vitro* electrophysiology experiments, respectively, and wrote the manuscript. M.M.-L., A.B.-G., L.B., M.V., and E.S.-G. contributed to behavioral experiments. A.A. and M.M.-F. provided calcium measurements. B.B., I.S., A.V.E., I.M., G.B., and I.B. contributed to the measurements of amino acids. F.D. supervised part of the work. T.P. and M.W.S. helped with *in vitro* electrophysiology. F.G. supervised *in vivo* electrophysiology. A.P. and S.H.R.O. supervised *in vitro* electrophysiology. G.M. conceived and supervised the whole project and wrote the manuscript. All authors edited and approved the manuscript.

DECLARATION OF INTERESTS

The authors declare no competing interests.

Received: April 6, 2017

Revised: March 20, 2018

Accepted: April 24, 2018

Published: May 17, 2018

REFERENCES

- Adage, T., Trillat, A.C., Quattropani, A., Perrin, D., Cavarec, L., Shaw, J., Guerassimenko, O., Giachetti, C., Gréco, B., Chumakov, I., et al. (2008). *In vitro* and *in vivo* pharmacological profile of AS057278, a selective d-amino acid oxidase inhibitor with potential anti-psychotic properties. *Eur. Neuropsychopharmacol.* **18**, 200–214.
- Allaman, I., Bélanger, M., and Magistretti, P.J. (2011). Astrocyte-neuron metabolic relationships: for better and for worse. *Trends Neurosci.* **34**, 76–87.
- Andersen, P. (2007). *The Hippocampus Book* (Oxford University Press).
- Andrade-Talavera, Y., Duque-Feria, P., Paulsen, O., and Rodríguez-Moreno, A. (2016). Presynaptic spike timing-dependent long-term depression in the mouse hippocampus. *Cereb. Cortex* **26**, 3637–3654.
- Araque, A., Carmignoto, G., Haydon, P.G., Oliet, S.H., Robitaille, R., and Volterra, A. (2014). Gliotransmitters travel in time and space. *Neuron* **81**, 728–739.
- Araque, A., Castillo, P.E., Manzoni, O.J., and Tonini, R. (2017). Synaptic functions of endocannabinoid signaling in health and disease. *Neuropharmacology* **124**, 13–24.
- Balderas, I., Rodríguez-Ortiz, C.J., and Bermudez-Rattoni, F. (2015). Consolidation and reconsolidation of object recognition memory. *Behav. Brain Res.* **285**, 213–222.
- Bohmbach, K., Schwarz, M.K., Schoch, S., and Henneberger, C. (2018). The structural and functional evidence for vesicular release from astrocytes *in situ*. *Brain Res. Bull.* **136**, 65–75.
- Boite, S., and Cordelières, F.P. (2006). A guided tour into subcellular colocalization analysis in light microscopy. *J. Microsc.* **224**, 213–232.
- Bosier, B., Bellocchio, L., Metna-Laurent, M., Soria-Gomez, E., Matias, I., Hebert-Chatelain, E., Cannich, A., Maitre, M., Leste-Lasserre, T., Cardinal, P., et al. (2013). Astroglial CB1 cannabinoid receptors regulate leptin signaling in mouse brain astrocytes. *Mol. Metab.* **2**, 393–404.
- Bushong, E.A., Martone, M.E., Jones, Y.Z., and Ellisman, M.H. (2002). Protoplasmic astrocytes in CA1 stratum radiatum occupy separate anatomical domains. *J. Neurosci.* **22**, 183–192.
- Busquets-García, A., Puighermanal, E., Pastor, A., de la Torre, R., Maldonado, R., and Ozaita, A. (2011). Differential role of anandamide and 2-arachidonoylglycerol in memory and anxiety-like responses. *Biol. Psychiatry* **70**, 479–486.
- Busquets-García, A., Gomis-González, M., Guegan, T., Agustín-Pavón, C., Pastor, A., Mato, S., Pérez-Samartín, A., Matute, C., de la Torre, R., Dierssen, M., et al. (2013). Targeting the endocannabinoid system in the treatment of fragile X syndrome. *Nat. Med.* **19**, 603–607.
- Busquets-García, A., Desprez, T., Metna-Laurent, M., Bellocchio, L., Marsicano, G., and Soria-Gomez, E. (2015). Dissecting the cannabinergic control of behavior: the where matters. *BioEssays* **37**, 1215–1225.
- Busquets Garcia, A., Soria-Gomez, E., Bellocchio, L., and Marsicano, G. (2016). Cannabinoid receptor type-1: breaking the dogmas. *F1000Res.* **5**, 5.
- Busquets-García, A., Bains, J., and Marsicano, G. (2018). CB₁ receptor signaling in the brain: extracting specificity from ubiquity. *Neuropsychopharmacology* **43**, 4–20.
- Castillo, P.E., Younts, T.J., Chávez, A.E., and Hashimoto, Y. (2012). Endocannabinoid signaling and synaptic function. *Neuron* **76**, 70–81.
- Chevalyère, V., and Castillo, P.E. (2003). Heterosynaptic LTD of hippocampal GABAergic synapses: a novel role of endocannabinoids in regulating excitability. *Neuron* **38**, 461–472.
- Fukushima, T., Kawai, J., Imai, K., and Toyo'oka, T. (2004). Simultaneous determination of D- and L-serine in rat brain microdialysis sample using a column-switching HPLC with fluorimetric detection. *Biomed. Chromatogr.* **18**, 813–819.
- Galve-Roperh, I., Aguado, T., Palazuelos, J., and Guzmán, M. (2007). The endocannabinoid system and neurogenesis in health and disease. *Neuroscientist* **13**, 109–114.
- Gómez-Gonzalo, M., Navarrete, M., Perea, G., Covelo, A., Martín-Fernández, M., Shigemoto, R., Luján, R., and Araque, A. (2015). Endocannabinoids induce lateral long-term potentiation of transmitter release by stimulation of gliotransmission. *Cereb. Cortex* **25**, 3699–3712.
- Han, J., Kesner, P., Metna-Laurent, M., Duan, T., Xu, L., Georges, F., Koehl, M., Abrous, D.N., Mendizabal-Zubiaga, J., Grandes, P., et al. (2012). Acute cannabinoids impair working memory through astroglial CB1 receptor modulation of hippocampal LTD. *Cell* **148**, 1039–1050.
- Hebert-Chatelain, E., Desprez, T., Serrat, R., Bellocchio, L., Soria-Gomez, E., Busquets-García, A., Pagano Zottola, A.C., Delamarre, A., Cannich, A., Vincent, P., et al. (2016). A cannabinoid link between mitochondria and memory. *Nature* **539**, 555–559.
- Henneberger, C., Papouin, T., Oliet, S.H., and Rusakov, D.A. (2010). Long-term potentiation depends on release of D-serine from astrocytes. *Nature* **463**, 232–236.
- Hirrlinger, P.G., Scheller, A., Braun, C., Hirrlinger, J., and Kirchhoff, F. (2006). Temporal control of gene recombination in astrocytes by transgenic expression of the tamoxifen-inducible DNA recombinase variant CreERT2. *Glia* **54**, 11–20.
- Kandel, E.R., Schwartz, J.H., Jessel, T.M., Siegelbaum, S.A., and Hudspeth, A.J. (2002). *Principles of Neural Science, Fifth Edition* (McGraw-Hill Professional).

- Kano, M., Ohno-Shosaku, T., Hashimoto-dani, Y., Uchigashima, M., and Watanabe, M. (2009). Endocannabinoid-mediated control of synaptic transmission. *Physiol. Rev.* **89**, 309–380.
- Marsicano, G., and Lafenêtre, P. (2009). Roles of the endocannabinoid system in learning and memory. *Curr. Top. Behav. Neurosci.* **1**, 201–230.
- Marsicano, G., Goodenough, S., Monory, K., Hermann, H., Eder, M., Cannich, A., Azad, S.C., Cascio, M.G., Gutiérrez, S.O., van der Stelt, M., et al. (2003). CB1 cannabinoid receptors and on-demand defense against excitotoxicity. *Science* **302**, 84–88.
- Martín, R., Bajo-Grañeras, R., Moratalla, R., Perea, G., and Araque, A. (2015). Circuit-specific signaling in astrocyte-neuron networks in basal ganglia pathways. *Science* **349**, 730–734.
- Martin-Fernandez, M., Jamison, S., Robin, L.M., Zhao, Z., Martin, E.D., Aguilar, J., Benneyworth, M.A., Marsicano, G., and Araque, A. (2017). Synapse-specific astrocyte gating of amygdala-related behavior. *Nat. Neurosci.* **20**, 1540–1548.
- Massa, F., Koehl, M., Wiesner, T., Grosjean, N., Revest, J.M., Piazza, P.V., Abrous, D.N., and Oliet, S.H. (2011). Conditional reduction of adult neurogenesis impairs bidirectional hippocampal synaptic plasticity. *Proc. Natl. Acad. Sci. USA* **108**, 6644–6649.
- Metna-Laurent, M., and Marsicano, G. (2015). Rising stars: modulation of brain functions by astroglial type-1 cannabinoid receptors. *Glia* **63**, 353–364.
- Min, R., and Nevian, T. (2012). Astrocyte signaling controls spike timing-dependent depression at neocortical synapses. *Nat. Neurosci.* **15**, 746–753.
- Monory, K., Polack, M., Remus, A., Lutz, B., and Korte, M. (2015). Cannabinoid CB1 receptor calibrates excitatory synaptic balance in the mouse hippocampus. *J. Neurosci.* **35**, 3842–3850.
- Navarrete, M., and Araque, A. (2008). Endocannabinoids mediate neuron-astrocyte communication. *Neuron* **57**, 883–893.
- Navarrete, M., and Araque, A. (2010). Endocannabinoids potentiate synaptic transmission through stimulation of astrocytes. *Neuron* **68**, 113–126.
- Oliveira da Cruz, J.F., Robin, L.M., Drago, F., Marsicano, G., and Metna-Laurent, M. (2016). Astroglial type-1 cannabinoid receptor (CB1): a new player in the tripartite synapse. *Neuroscience* **323**, 35–42.
- Panatier, A., and Oliet, S.H. (2006). Neuron-glia interactions in the hypothalamus. *Neuron Glia Biol.* **2**, 51–58.
- Panatier, A., Theodosis, D.T., Mothet, J.P., Touquet, B., Pollegioni, L., Poulain, D.A., and Oliet, S.H. (2006). Glia-derived D-serine controls NMDA receptor activity and synaptic memory. *Cell* **125**, 775–784.
- Pannasch, U., and Rouach, N. (2013). Emerging role for astroglial networks in information processing: from synapse to behavior. *Trends Neurosci.* **36**, 405–417.
- Papouin, T., Ladépêche, L., Ruel, J., Sacchi, S., Labasque, M., Hanini, M., Groc, L., Pollegioni, L., Mothet, J.P., and Oliet, S.H. (2012). Synaptic and extrasynaptic NMDA receptors are gated by different endogenous coagonists. *Cell* **150**, 633–646.
- Papouin, T., Dunphy, J., Tolman, M., Foley, J.C., and Haydon, P.G. (2017a). Astrocytic control of synaptic function. *Philos. Trans. R. Soc. Lond. B Biol. Sci.* **372**, 372.
- Papouin, T., Dunphy, J.M., Tolman, M., Dineley, K.T., and Haydon, P.G. (2017b). Septal cholinergic neuromodulation tunes the astrocyte-dependent gating of hippocampal NMDA receptors to wakefulness. *Neuron* **94**, 840–854.e7.
- Papouin, T., Henneberger, C., Rusakov, D.A., and Oliet, S.H.R. (2017c). Astroglial versus neuronal D-serine: fact checking. *Trends Neurosci.* **40**, 517–520.
- Paxinos, G., and Franklin, K.B.J. (2001). *The Mouse Brain in Stereotaxic Coordinates* (Academic Press).
- Perea, G., and Araque, A. (2005). Properties of synaptically evoked astrocyte calcium signal reveal synaptic information processing by astrocytes. *J. Neurosci.* **25**, 2192–2203.
- Perea, G., Navarrete, M., and Araque, A. (2009). Tripartite synapses: astrocytes process and control synaptic information. *Trends Neurosci.* **32**, 421–431.
- Piomelli, D. (2003). The molecular logic of endocannabinoid signalling. *Nat. Rev. Neurosci.* **4**, 873–884.
- Porter, J.T., and McCarthy, K.D. (1996). Hippocampal astrocytes in situ respond to glutamate released from synaptic terminals. *J. Neurosci.* **16**, 5073–5081.
- Puighermanal, E., Marsicano, G., Busquets-Garcia, A., Lutz, B., Maldonado, R., and Ozaita, A. (2009). Cannabinoid modulation of hippocampal long-term memory is mediated by mTOR signaling. *Nat. Neurosci.* **12**, 1152–1158.
- Puighermanal, E., Busquets-Garcia, A., Gomis-González, M., Marsicano, G., Maldonado, R., and Ozaita, A. (2013). Dissociation of the pharmacological effects of THC by mTOR blockade. *Neuropsychopharmacology* **38**, 1334–1343.
- Rasooli-Nejad, S., Palygin, O., Lalo, U., and Pankratov, Y. (2014). Cannabinoid receptors contribute to astroglial Ca²⁺-signalling and control of synaptic plasticity in the neocortex. *Philos. Trans. R. Soc. Lond. B Biol. Sci.* **369**, 20140077.
- Rothman, J.S., and Silver, R.A. (2018). NeuroMatic: an integrated open-source software toolkit for acquisition, analysis and simulation of electrophysiological data. *Front. Neuroinform.* Published online April 4, 2018. <https://doi.org/10.3389/fninf.2018.00014>.
- Sherwood, M.W., Arizono, M., Hisatsune, C., Bannai, H., Ebisui, E., Sherwood, J.L., Panatier, A., Oliet, S.H., and Mikoshiba, K. (2017). Astrocytic IP₃ Rs: contribution to Ca²⁺ signalling and hippocampal LTP. *Glia* **65**, 502–513.
- Shigetomi, E., Jackson-Weaver, O., Huckstepp, R.T., O'Dell, T.J., and Khakh, B.S. (2013). TRPA1 channels are regulators of astrocyte basal calcium levels and long-term potentiation via constitutive D-serine release. *J. Neurosci.* **33**, 10143–10153.
- Soria-Gómez, E., Bellocchio, L., Reguero, L., Lepousez, G., Martin, C., Bendahmane, M., Ruehle, S., Remmers, F., Desprez, T., Matias, I., et al. (2014). The endocannabinoid system controls food intake via olfactory processes. *Nat. Neurosci.* **17**, 407–415.
- Soria-Gómez, E., Busquets-Garcia, A., Hu, F., Mehidi, A., Cannich, A., Roux, L., Louit, I., Alonso, L., Wiesner, T., Georges, F., et al. (2015). Habenular CB1 receptors control the expression of aversive memories. *Neuron* **88**, 306–313.
- Sultan, S., Li, L., Moss, J., Petrelli, F., Cassé, F., Gebara, E., Lopatar, J., Pfrieger, F.W., Bezzi, P., Bischofberger, J., and Toni, N. (2015). Synaptic integration of adult-born hippocampal neurons is locally controlled by astrocytes. *Neuron* **88**, 957–972.
- Warburton, E.C., and Brown, M.W. (2015). Neural circuitry for rat recognition memory. *Behav. Brain Res.* **285**, 131–139.
- Warburton, E.C., Barker, G.R., and Brown, M.W. (2013). Investigations into the involvement of NMDA mechanisms in recognition memory. *Neuropharmacology* **74**, 41–47.
- Whitlock, J.R., Heynen, A.J., Shuler, M.G., and Bear, M.F. (2006). Learning induces long-term potentiation in the hippocampus. *Science* **313**, 1093–1097.
- Windels, F. (2006). Neuronal activity: from in vitro preparation to behaving animals. *Mol. Neurobiol.* **34**, 1–26.
- Wolosker, H., Balu, D.T., and Coyle, J.T. (2016). The rise and fall of the d-serine-mediated gliotransmission hypothesis. *Trends Neurosci.* **39**, 712–721.

STAR★METHODS

KEY RESOURCES TABLE

REAGENT or RESOURCE	SOURCE	IDENTIFIER
Antibodies		
Mouse anti-NeuN antibody	Millipore	Cat# MAB377; RRID: AB_2298772
Rabbit anti-s100 β antibody	Sigma-Aldrich	Cat# HPA015768; RRID: AB_1856538
Donkey anti-mouse Alexa 647	Thermo Fisher Scientific	Cat# 10226162; RRID: AB_895335
Donkey anti-rabbit Alexa 488	Thermo Fisher Scientific	Cat# 10424752; RRID: AB_1623506
Bacterial and Virus Strains		
Viral Vector: AAV-GFAP-GFP	This paper	Virus n52 lab stock
Viral Vector: AAV-GFAP-CRE-mCherry	UNC Vector Core	N/A
Chemicals, Peptides, and Recombinant Proteins		
2,3-Naphthalenedicarboxaldehyde (NDA)	Fluka	Cat# 70215, CAS: 7149-49-7
AM251	Tocris	Cat# 1117
AS057278	Sigma-Aldrich	Cat# 644927
D-AP5	Sigma-Aldrich	Cat# A8054
DMSO	Sigma-Aldrich	Cat# D5879-M
D-serine	Ascent Scientific	Cat# ab120048
Fluo-4 AM	Thermo Fisher Scientific	Cat# F14201
Glutamate	Sigma-Aldrich	Cat# 49621, CAS: 6106-04-3
Glycine	Sigma-Aldrich	Cat# G7126, CAS: 56-40-6
Isoflurane	Virbac	N/A
Ketamine (IMALGENE 500)	Merial	N/A
Lidocaine (Lurocaine)	Vetoquinol	N/A
LY367385	Abcam	Cat# ab120067
MK-801	Abcam	Cat# ab120027
MTEP	Tocris	Cat# 2921
NBQX	Tocris	Cat# 1044
Paraformaldehyde	Sigma-Aldrich	Cat# HT501128
SR101	Sigma-Aldrich	Cat# S7635
Tamoxifen	Sigma-Aldrich	Cat# T5648
TTX	Tocris	Cat# 1078
Xylazine (ROMPUN)	Bayer	N/A
WIN 515,212-2	Sigma-Aldrich	Cat# W102
γ -Aminobutyric acid (GABA)	Sigma-Aldrich	Cat# A2129, CAS: 56-12-2
Critical Commercial Assays		
Pierce BCA Protein Assay Kit	Thermo Fisher Scientific	Cat# 23225
Experimental Models: Organisms/Strains		
Mouse: C57BL/6N	JANVIER Labs	C57BL/6NRj
Mouse: <i>CB₁</i> -flox	Marsicano et al., 2003	N/A
Mouse: GFAP- <i>CB₁</i> -KO	Han et al., 2012	N/A
Software and Algorithms		
Axoclamp 900A	Molecular Devices	N/A
Axon pClamp10	Molecular Devices	N/A
Behavioral Scoring Panel	A. Dubreucq	N/A
GraphPad Prism 6.0	GraphPad Software	N/A
ImageJ	NIH	N/A

(Continued on next page)

Continued

REAGENT or RESOURCE	SOURCE	IDENTIFIER
IGOR Pro v.6.37	WaveMetrics	N/A
Karat 32 software v.8.0	Beckman Coulter	N/A
NeuroMatic v.2.8t	Rothman and Silver, 2018	N/A
Spike2	Cambridge Electronic Design	N/A

CONTACT FOR REAGENT AND RESOURCE SHARING

Further information and requests for resources should be directed to the Lead Contact Giovanni Marsicano (giovanni.marsicano@inserm.fr).

EXPERIMENTAL MODEL AND SUBJECT DETAILS**Animals**

All experiments were conducted in strict compliance with the European Union recommendations (2010/63/EU) and were approved by the French Ministry of Agriculture and Fisheries (authorization number 3306369) and the local ethical committee (authorization number A50120118). Two to three months-old naive male C57BL/6N (JANVIER, France), CB_1 -flox (mice carrying the “floxed” CB_1 gene ($CB1^{f/f}$)) and male GFAP- CB_1 -KO mutant mice and GFAP- CB_1 -WT littermates were used. Animals were housed in groups under standard conditions in a day/night cycle of 12/12 hr (light on at 7 am). Behavioral experiments were conducted between 2 and 5 pm. *In vivo* electrophysiological experiments were conducted during the light phase. Mice undergoing surgery were housed individually after the procedure.

GFAP- CB_1 -KO mice were generated using the CRE/loxP system as previously described ([Han et al., 2012](#)). Mice carrying the “floxed” CB_1 gene ($CB1^{f/f}$) ([Marsicano et al., 2003](#)) were crossed with GFAP-CreERT2 mice ([Hirrlinger et al., 2006](#)), using a three-step backcrossing procedure to obtain $CB_1^{f/f;GFAP-CreERT2}$ and $CB_1^{f/f}$ littermates, called GFAP- CB_1 -KO and GFAP- CB_1 -WT, respectively. As CreERT2 protein is inactive in the absence of tamoxifen treatment ([Hirrlinger et al., 2006](#)), deletion of the CB_1 gene was obtained in adult mice (7-9 weeks-old) by daily i.p. injections of tamoxifen (1 mg dissolved at 10 mg/mL in 90% sesame oil, 10% ethanol, Sigma-Aldrich, France) for 8 days. Mice were used 3-5 weeks after the last tamoxifen injection ([Han et al., 2012](#)).

METHOD DETAILS**Drug Preparation and Administration**

For behavioral experiments, D-serine (Ascent Scientific, United Kingdom) was dissolved in 0.9% saline for systemic injections in order to inject 10 mL/kg of body weight in each mouse. For intra-hippocampal infusions, D-serine was dissolved in artificial cerebrospinal fluid (aCSF). AS057278 (Sigma-Aldrich, France) was dissolved in 0.9% saline added with 2% DMSO, 10% ethanol. D-AP5 (Sigma-Aldrich, France) was dissolved in aCSF. All vehicles contained the same amounts of solvents. All drugs were prepared freshly before the experiments. All drugs were injected either intraperitoneally (i.p.) or intra-hippocampally immediately after the acquisition phase of the NOR task (see below for exceptions), except for AS057278, which was injected 2 hr before, based on published data indicating the peak of endogenous D-serine at this time point ([Adage et al., 2008](#)). D-serine was also intraperitoneally injected 1 hr after the acquisition and right before the test session. D-AP5 was also injected intra-hippocampally 6 hr after the acquisition.

Intra-hippocampal drug infusions (see below) were performed with the aid of 30-gauge injectors protruding 1.0 mm from the end of the cannulae. The volume infused was: 0.3 μ L at a rate of 0.3 μ L/min. After infusion, injectors were kept in place for 60 s to prevent outflow of injected solutions.

Intra-hippocampal Drug Delivery

Mice (8-12 weeks of age) were anesthetized by intraperitoneal injection of a mixture of ketamine (100mg/kg, Imalgene 500, Merial, France) and Xylazine (10mg/kg, Rompun, Bayer, France) and placed into a stereotaxic apparatus (David Kopf Instruments, CA, USA) with mouse adaptor and lateral ear bars. For intra-hippocampal infusions of drugs, mice were bilaterally implanted with 23-gauge stainless steel guide cannulae (Bilaney, Germany) following stereotaxic coordinates ([Paxinos and Franklin, 2001](#)) aiming at the dorsal hippocampus (AP – 1.8, ML \pm 1, DV – 1.3 mm), guide cannulae were secured with cement anchored to the skull by screws. Mice were allowed to recover for at least one week in individual cages before the beginning of the experiments. During the recovery period, mice were handled daily.

Viral Vectors, Intra-hippocampal Delivery, and Histological Verification

AAV-GFAP-GFP control virus was produced in the lab as previously described (Hebert-Chatelain et al., 2016; Soria-Gómez et al., 2014, 2015) by using pAAV-GFAP-EGFP plasmid (ADDGENE #50473) as vector backbone. AAV-GFAP-CRE-mCherry was acquired from UNC vector core (NC, USA). Both viral vectors were rAAV serotype 8 with titers 4.17×10^{11} for AAV-GFAP-GFP and 1.2×10^{12} for AAV-GFAP-CRE-mCherry, respectively. For viral intra-HPC AAV delivery, mice were submitted to stereotaxic surgery (as above) and AAV vectors were injected with the help of a microsyringe (0.25 mL Hamilton syringe with a 30-gauge beveled needle) attached to a pump (UMP3-1, World Precision Instruments, FL, USA). Mice were injected directly into the hippocampus (HPC) (0.5 μ L per injection site at a rate of 0.5 μ L per min), with the following coordinates: dorsal HPC, AP -1.8 ; ML ± 1 ; DV -2.0 and -1.5 ; ventral HPC: AP -3.5 ; ML ± 2.7 ; DV -4 and -3 . Following virus delivery, the syringe was left in place for 1 min before being slowly withdrawn from the brain. *CB₁*-flox mice were injected with AAV-GFAP-GFP (control) or AAV-GFAP-CRE (fused to mCherry, serotype 8, UNC Vector Core, USA) to induce deletion of the *CB₁* gene in hippocampal astroglial cells. Animals were used for experiments 4-5 weeks after injections. Mice were weighed daily and individuals that failed to regain the pre-surgery body weight were excluded from the following experiments. To verify the correct pattern of CRE expression and localization, mice were transcardially perfused with paraformaldehyde (Sigma Aldrich, France) and their brains were sliced with a vibratome. 40 μ m hippocampal sections incubated with primary antibody directed against s100 β (Rabbit polyclonal, Sigma Aldrich, France) and NeuN (Mouse monoclonal, Millipore, France). Secondary antibodies incubation was performed in order to detect s100 β with Alexa 488 (Thermo Scientific, France) and NeuN with Alexa 647 (Thermo Scientific, France). Single plane confocal images were acquired with an SP8 confocal microscope (Leica, France) and minimally processed with ImageJ software. Automatic quantification of mCherry (CRE positive), s100 β and NeuN expressing cells was performed with ImageJ software as previously described (Bolte and Cordelières, 2006). Briefly, after threshold subtraction and crosstalk correction, the number of cells co-expressing mCherry/s100 β or mCherry/NeuN was automatically obtained by the “particle analysis” tool of the same software. mCherry/s100 β co-expressing cells were expressed in percentage of CRE positive cells as well as percentage of total s100 β cells. On the other hand, mCherry/NeuN co-expressing cells were reported as percentage of CRE positive cells as well as percentage of total NeuN cells.

Novel Object Recognition Memory Task

We used the novel object recognition memory task in a L-maze (NOR) (Busquets-Garcia et al., 2011, 2013; Puighermanal et al., 2009, 2013). As compared to other hippocampal-dependent memory tasks, this test presents several advantages for the aims of the present study: (i) the acquisition of NOR occurs in one step and previous studies revealed that the consolidation of this type of memory is deeply altered by acute immediate post-training administration of cannabinoids via hippocampal *CB₁* receptors (Puighermanal et al., 2009, 2013); (ii) the NOR test performed in a L-maze decrease variability and give strong and replicable results; (iii) this test allows repeated independent measurements of memory performance in individual animals (Puighermanal et al., 2013), thereby allowing within-subject comparisons, eventually excluding potential individual differences in viral infection.

The task took place in a L-shaped maze made of dark gray polyvinyl chloride shaped by two identical perpendicular arms (35 cm and 30 cm long respectively for external and internal L walls, 4.5 cm wide and 15 cm high walls) placed on a white background (Busquets-Garcia et al., 2011; Puighermanal et al., 2009). The task occurred in a room adjacent to the animal house with a light intensity fixed at 50 lux. The maze was overhung by a video camera allowing the detection and scoring offline of animal's behavior.

The task consisted of 3 sequential daily trials of 9 min each. During the habituation session (day 1), mice were placed in the center of the maze and allowed to freely explore the arms in the absence of any objects. The acquisition session (day 2) consisted in placing the mice again in the center of the maze in the presence of two identical objects positioned at the extremities of each arm and left to freely explore the maze and the objects. The memory test occurred 24 hr later (day 3): one of the familiar objects was replaced by a novel object different in its shape, color, and texture and mice were left to explore both objects. The position of the novel object and the associations of novel and familiar were randomized. All objects were previously tested to avoid biased preference. The apparatus as well as objects were cleaned with ethanol (70%) before experimental use and between each animal testing. Memory performance was assessed by the discrimination index (DI). The DI was calculated as the difference between the time spent exploring the novel (TN) and the familiar object (TF) divided by the total exploration time (TN+TF): $DI = [TN - TF] / [TN + TF]$. Memory was also evaluated by directly comparing the exploration time of novel and familiar objects, respectively. Object exploration was defined as the orientation of the nose to the object at a distance of less than 2 cm. Experienced investigators evaluating the exploration were blind to the treatment and/or genotype of the animals.

In Vivo Electrophysiology

GFAP-*CB₁*-KO and WT littermate mice were anesthetized in a box containing 5% Isoflurane (Virbac, France) before being placed in a stereotaxic frame (model SR-6M-HT, Narishige International, United Kingdom) in which 1.0% to 1.5% of Isoflurane was continuously supplied via an anesthetic mask during the complete duration of the experiment. The body temperature was maintained at 37°C using a homeothermic system (model 50-7087-F, Harvard Apparatus, MA, USA) and the complete state of anesthesia was assured through a mild tail pinch. Before surgery, 100 μ L of the local anesthetic Lurocaine (Vetoquinol, France) was injected in the scalp region. Surgical procedure started with a longitudinal incision of 1.5 cm in length aimed to expose Bregma and Lambda. After ensuring correct alignment of the head, two holes were drilled in the skull to place: a glass recording electrode, inserted in the CA1 *stratum radiatum*, and one concentric bipolar electrode (Model NE-100, KOPF Instruments, Tujunga, CA, USA) in the CA3 region using the following

coordinates: 1) CA1 *stratum radiatum*: A/P -1.5 mm, M/L -1.0 mm, DV 1.20 mm; CA3: A/P -2.5 mm, M/L -2.8 , D/V -2.0 mm. The recording electrode (tip diameter = $1-2$ μm , $4-6$ M Ω) was filled with a 2% pontamine sky blue solution in 0.5M sodium acetate. At first the recording electrode was placed by hand until it reached the surface of the brain and then to the final depth using an automatic micropositioner (MIM100-2, M2E, France). The stimulation electrode was placed in the correct area using a micromanipulator (UNI-Z, M2E, France). Both electrodes were adjusted to find the area with maximum response. *In vivo* recordings of evoked field excitatory postsynaptic potentials (fEPSPs) were amplified 10 times by Axoclamp 900A amplifier (Molecular Devices, CA, USA) before being further amplified 100 times and filtered (low pass at 1 Hz and high-pass at 5000Hz) via a differential AC amplifier (model 1700; A-M Systems, Sequim, WA, USA). fEPSPs were digitized and collected on-line using a laboratory interface and software (CED 1401, SPIKE 2; Cambridge Electronic Design, UK). Test pulses were generated through an Isolated Constant Current Stimulator (DS3, Digitimer, UK) triggered by the SPIKE 2 output sequencer via CED 1401 and collected every 2 s at a 10 kHz sampling frequency and then averaged every 300 s. Test pulse intensities were typically between 50–250 μA with a duration of 500 μs . Basal stimulation intensity was adjusted to 30%–40% of the current intensity that evoked a maximum field response. All responses were expressed as percent from the average responses recorded during the 10 min before high-frequency stimulation (HFS). HFS was induced by applying 3 trains of 100 Hz (1 s each), separated by 20 s interval. fEPSP were then recorded for a period of 40 min. In the specific group of mice the following treatments were applied: 1) MK-801 (Abcam, United Kingdom; 3 mg/kg, i.p., dissolved in saline, approx. 60 min before HFS) or vehicle (saline, i.p., approx. 60 min before HFS) 2) D-serine (Ascent Scientific, United Kingdom; 50 mg/kg, i.p., dissolved in saline) approx. 2 hr before HFS or vehicle (saline, i.p.). At the end of each experiment, the positions of the electrodes were marked by iontophoretic infusion of the recording solution during 180 s at -20 μA and continuous current discharge over 20 s at $+20$ μA for recording and stimulation areas, respectively. Histological verification was performed *ex vivo*.

In Vitro Electrophysiology

Coronal hippocampal slices (350 μm) were prepared from adult GFAP-*CB1*-WT or GFAP-*CB1*-KO mice as described previously (Papouin et al., 2012). Briefly, mice were anesthetized with isoflurane and then decapitated. The brain was quickly extracted and placed in aCSF saturated with 95% O₂ and 5% CO₂. aCSF contained (in mM): 125 NaCl, 2.5 KCl, 1 Na₂HPO₄, 1.2 MgCl₂, 0.6 CaCl₂, 26 NaHCO₃ and 11 mM glucose (pH 7.4; 300 mosmol/kg). Coronal slices were cut from a block of tissue containing the hippocampus using a vibratome (Microm HM 650V, Thermo Scientific, USA). Slices were hemisected and maintained at 33°C during 30 min in aCSF containing 2 mM MgCl₂ and 1 mM CaCl₂. Then, they were allowed to recover at room temperature for at least 1 hr.

Slices were transferred into a recording chamber perfused with aCSF (2.8 mL/min) containing 1.3 mM MgCl₂ and 2.5 mM CaCl₂, and maintained at 30°C. fEPSPs slope were recorded with a Multiclamp 700A amplifier (Molecular Devices, CA, USA), using pipettes (2–3 M Ω) filled with aCSF and placed in the *stratum radiatum* of CA1 area. Synaptic responses were evoked at 0.05 Hz by orthodromic stimulation (100 μs duration) of Schaffer collaterals using a concentric bipolar tungsten electrode placed >200 μm away from the recording electrodes. For LTP experiments, stimulation intensity was set to 35% of that triggering population spikes. After a stable baseline of at least 10 min, LTP was induced by applying a HFS protocol consisting of a 100 Hz train of stimuli for 1 s repeated three times at 20 s intervals. MTEP (500 nM; 500 μM stock in dH₂O; Tocris, United Kingdom) and LY367385 (100 μM ; 100 mM stock in 1.1e^q NaOH; Abcam, United Kingdom), or the vehicle control, were perfused after a stable baseline of at least 10 min. To inhibit mGluR1/5 during LTP induction, MTEP and LY367385 were perfused for 20 min prior to LTP induction and removed 2 min post-LTP induction. NMDAR-fEPSPs were recorded in low Mg²⁺ aCSF (0.2 mM) with 2,3-dihydroxy-6-nitro-7-sulfamoyl-benzo[f]quinoxaline-2,3-dione (NBQX; 10 μM , Tocris, United Kingdom) to block AMPA/kainate receptors. At the end of each experiment, D-AP5 (50 μM , Sigma-Aldrich, France), was applied to isolate the remaining GABAergic component which was then subtracted from the responses to obtain pure NMDAR-fEPSPs. Average fEPSP and NMDAR-fEPSP traces correspond to 10 min and 20 min of stable recording, respectively. For clarity the stimulation artifact was deleted.

Signals were filtered at 2 kHz and digitized at 10 kHz. Data were collected and analyzed using pClamp10 software (Molecular Devices, CA, USA).

Ca²⁺ Imaging

Ca²⁺ levels in astrocytes located in the *stratum radiatum* of the CA1 region of the hippocampus were monitored by fluorescence microscopy using the Ca²⁺ indicator fluo-4 AM (Thermo fisher scientific, MA, USA). Slices were incubated with fluo-4 AM (2 μL of 2 mM dye were dropped over the hippocampus, attaining a final concentration of 2 μM and 0.01% of pluronic) for 20–30 min at room temperature. In these conditions, most of the cells loaded were astrocytes, as confirmed by their electrophysiological properties and SR101 (Sigma-Aldrich, USA) staining. Astrocytes were imaged using a Leica SP5 multiphoton microscope and images were acquired at 1 to 2 Hz. Intracellular Ca²⁺ signals were monitored from astrocytic somas and processes and the signal was measured as fluorescence over baseline [(Fluorescence_t - Background fluorescence_t) - (Fluorescence₀ - Background fluorescence₀)] / (Fluorescence₀ - Background fluorescence₀) and cells were considered to display a Ca²⁺ event when the calcium signal increased three times the standard deviation of the baseline.

The astrocyte Ca²⁺ signal was quantified as the probability of occurrence of a Ca²⁺ event (calcium event probability). The Ca²⁺ event probability was calculated as the number of somas or processes starting a calcium event per time bin in a field of view, divided by the number of somas or processes in that field of view (8–12 somas and 15–20 processes in each field of view). Events were grouped in 10 s time bins. The time of occurrence of an event was considered to be at the onset of the Ca²⁺ event. The calcium event

probability during 20 s before the WIN 515,212-2 (WIN, Sigma-Aldrich, USA) application (200 μ M, 3 s, 10 psi) was compared with the calcium event probability in the time bin after the WIN application. WIN was dissolved in DMSO and then 36 μ L of the DMSO-WIN solution was diluted in 1 mL of aCSF, obtaining a final concentration of 200 μ M used in the pressure-pulse pipette. We estimate, based on quantifications of Alexa 594 fluorescence, that the WIN concentration becomes further diluted after being pressure ejected in the bath aCSF to approximately 1-10 μ M around the recorded cells (Navarrete and Araque, 2008). In some cases, experiments were performed in the presence of the CB₁ antagonist AM251 (2 μ M, Tocris, United Kingdom). Mean values were obtained from at least 5 slices and 2 mice in each condition.

Measurement of Amino Acids in Hippocampal Slices

For the simultaneous measurement of D-serine, glutamate, glycine and GABA, a capillary electrophoresis-laser induced fluorescence detection method was used.

Five hippocampi from adult C57BL/6N mice (10-12 weeks old) were isolated from 350 μ m slices and incubated in 350 μ L oxygenated aCSF containing 0.5 μ M TTX (Tocris, United Kingdom) with either vehicle (1/4000 DMSO) or WIN (5 μ M in DMSO) during 30 min at 31°C. Extracellular medium was quickly removed, frozen using liquid nitrogen and stored at -80° C. Extracellular levels of D-serine, glutamate, glycine and GABA were then determined. Briefly, pooled slices were deproteinized by addition of cold trichloroacetic acid (TCA) to a 4% final concentration. The suspension was centrifuged at 16,800 g for 10 min, the TCA was extracted from the supernatant with water-saturated diethyl ether and stored at -80° C. Samples were analyzed with a commercial laser-induced fluorescence capillary electrophoresis (CE-LIF) (CE: Beckman Coulter (Brea, California, US), P/ACE MDQ; LIF: Picometrics (Labège, France), LIF-UV-02, 410 nm 20 mW) as following: samples were processed for micellar CE-LIF and were fluorescently derivatized at RT for 60 min with naphthalene-2,3-dicarboxaldehyde (NDA) before being analyzed by CE using a hydroxypropyl- β -cyclodextrin (HP-b-CD) based chiral separation buffer. All electropherograms data were collected and analyzed using Karat 32 software v8.0 (Beckman Coulter, France). The tissue amounts of D-serine, glutamate, glycine and GABA were normalized to the protein content determined from pooled hippocampal slices by the Lowry method using the BCA protein Pierce (ThermoScientific, CA, USA) assay with bovine serum albumin (BSA) as standards. The quantity of D-serine, glutamate, glycine and GABA in the samples was determined from a standardized curve while peak identification was made by spiking the fraction with the amino acid.

QUANTIFICATION AND STATISTICAL ANALYSIS

Data were expressed as mean \pm SEM or single data points and were analyzed with Prism 6.0 (Graphpad Software), using t test (paired or unpaired), Mann Whitney test or ANOVA (One- or Two-Way), where appropriate. Dunnet's, Holm-sidak (One-Way ANOVA) or Bonferroni's (Two-Way ANOVA) post hoc tests were used. Statistical details for each quantitative experiment are illustrated in [Table S1](#).